Desalination and Water Treatment
www.deswater.com

doi: 10.5004/dwt.2023.29478

290 (2023) 94–103
April

Estimation of evapotranspiration based on METRIC and SEBAL model using remote sensing, near Al-Jouf, Saudi Arabia

Esubalew Adem[a,b], Silvena Boteva[c], Lifu Zhang[d], Mohamed Elhag[a,d,e,f,*]

[a]*Department of Hydrology and Water Resources Management, Faculty of Meteorology, Environment and Arid Land Agriculture, King Abdulaziz University, Jeddah 21589, Saudi Arabia, email: melhag@kau.edu.sa (M. Elhag)*
[b]*Department of Geology, Faculty of Science, Arba Minch University, Arba Minch, Ethiopia*
[c]*Department of Ecology and Nature Conservation, Faculty of Biology, Sofia University "St. Kl. Ohridski", 8 Dragan Tsankov Blvd, 1164 Sofia, Bulgaria*
[d]*The State Key Laboratory of Remote Sensing, Aerospace Information Research Institute Chinese Academy of Science (CAS), Beijing 100101, China*
[e]*Department of Geoinformation in Environmental Management, CI-HEAM/Mediterranean Agronomic Institute of Chania, Chania 73100, Greece*
[f]*Department of Applied Geosciences, Faculty of Science, the German University of Technology in Oman, Muscat 1816, Oman*

Received 30 September 2022; Accepted 8 March 2023

ABSTRACT

The current study focuses on estimating evapotranspiration in arid and semi-arid environments in the Northern part of Saudi Arabia near Al-Jouf. The objective of the research is to study, analyze and estimate evapotranspiration (ET) using the surface energy balance algorithm for land (SEBAL) and mapping evapotranspiration at high resolution with internalized calibration (METRIC) model and compare the two models with vegetation index and land surface temperature. The image was processed in ArcGIS and MATLAB software with the toolbox LandMOD ET mapper. The area average evapotranspiration is about 2.21 mm/d for the METRIC model, 2.6 mm/d for SEBAL and the average land surface temperature is 324.3 K. ET and land surface temperature are highly inverse correlated, with an R^2 = 0.8. The value of ET ranges from 0.05 to 8 mm for both SEBAL and METRIC models during 2019/07/07. Both highly elevated and agricultural area shows a high value of ET ranging from 5 to 8 mm/d. In addition, the normalized differential vegetation index, leaf area index, and emissivity were also calculated from the surface energy balance equation. The estimation of ET from the SEBAL model is better than the METRIC model based on R^2 of different vegetation indices. The importance of the work is to estimate ET and explain the impact on environmental effects for better planning in water resource development.

Keywords: Evapotranspiration; Surface energy balance algorithm for land; Mapping evapotranspiration at high resolution with internalized calibration; Landsat; LandMOD mapper

1. Introduction

Evapotranspiration (ET) has played a significant role in the field of metrological and hydrological studies [1–3]. ET means the rate at which water detached from the various features of the earth's surface [4,5], that is, plant and soil expressed as the rate Le (latent heat flux) transfer per unit area (A) or the depth of water per unit time (t) removed from reference crop [6,7]. Nowadays in advanced remote sensing technology, Landsat images perform a good estimation of ET in arid and sub-arid environments [8,9]. According to Allen et al. [10], Anderson et al. [11] and Allen

* Corresponding author.

Presented at the 9th International Conference on Sustainable Solid Waste Management (CORFU 2022), June 15–18 2022, Corfu, Greece

1944-3994/1944-3986 © 2023 Desalination Publications. All rights reserved.

et al. [12], Landsat satellite image was used to calculate the mapping evapotranspiration at high resolution with internalized calibration (METRIC) model. Therefore, the model calculates evapotranspiration (ET), Le (latent heat flux), Ri (net radiation), (Gi) soil heat flux, and (Hi) sensible heat flux [13,14] of Al-Jouf area in Saudi Arabia.

Remote sensing methods and approaches to estimate evapotranspiration in a broad area is an important development in the hydrological field [15]. There are several methods to estimate and calculate ET [14,16–22]. Among these models, METRIC and surface energy balance algorithm for land (SEBAL) model uses satellite remote sensing data in terms of spatial and temporal resolution. One of the benefits of the METRIC model is that it has an autocalibration ability using ground-based calculation of alfalfa [23]. The surface energy balance algorithm for land (SEBAL) model was developed by the study of Bastiaanssen et al. [24], Which gained global attention in successful performance [25]. The METRIC model uses the SEBAL method for estimating radiometric surface temperature (d_T) [14]. Reference ET method where the crop coefficient (K_c) is related to vegetation indices obtained from canopy reflectance values [26,27]. ETr in METRIC model performs based on the principle of energy conservation [25].

ET is derived from the ratio between latent heat flux with the density of water (ϱ_w) and vaporization of latent heat [17,28]. In recent year, estimating energy balance by remote sensing techniques have become an important tool to estimate and evaluate the spatial and temporary variability of energy balance components [4,29], ET and crop coefficient (K_c) for complex canopy structures like orchards [17,30,31]. METRIC model has become a valued method to evaluate the spatial and temporary variability of ETa. Recently studies have been performed to compute potential evapotranspiration in various cities of the Kingdom of Saudi Arabia [32,33]. The climate condition of the region is characterized by arid and sub-arid conditions which are hot and dry summers with cool and slightly wet winters [27,34,35]. Potential evapotranspiration (ETr) estimation approaches that need only temperature as input data are considered temperature-based methods [36]. The temperature-based methods are some of the previous approaches for assessing ET [37]. According to Ramírez-Cuesta et al. [17] METRIC-GIS has been effectively tested and works in an arid and semi-arid region. Estimation of daily evapotranspiration was also tested over the Nile delta by surface energy balance system (SEBS) and evaporative fraction from remote sensing data [38,39]. The challenge of working with remote sensing images to estimate ET is difficult to collect reliable weather data [40] in image format for the process of METRIC and SEBAL model in LandMOD mapper in MATLAB software.

The objective of the analysis is to collect remote sensing Landsat 8 images to yield daily ET from METRIC and SEBAL models and compare them with different vegetation indices and land surface temperature (LST). The region is utilized for this study since it is an agricultural area located in the northern part of Saudi Arabia.

2. Materials and methods

2.1. Location of the region

The area is found in the northern part of Saudi Arabia between latitude 29° 30′ and 31° 30′ N and longitude 37° 00′ and 39° 00′ E and geographically located and bounded by Jordan to the North and from the South-Eastern border by Al-Jouf (Fig. 1). The area is covered by 27,364 km^2. The topographic feature is characterized by a mountainous region, which is mostly composed of agricultural areas and the

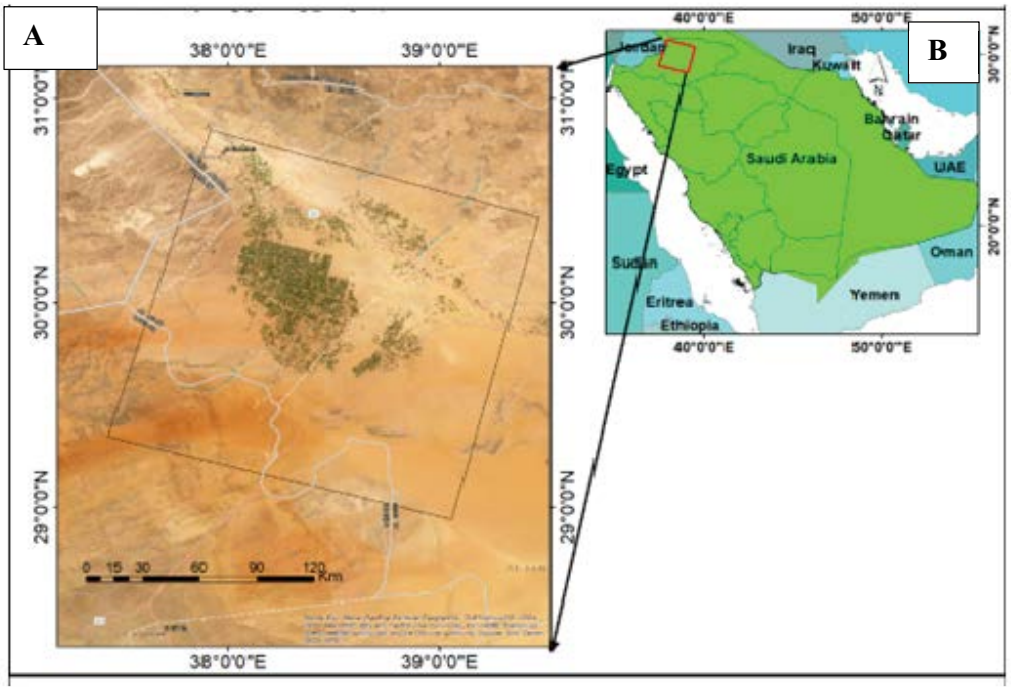

Fig. 1. (A) Map of the study area and (B) Location of Saudi Arabia, which depicted in green color.

other part is plateaus and valleys. The escarpment, which is the highest elevation measured about 1,047 m. The most important agricultural product of the study area and Al-Jouf contain date, grapes, and fruits like citrus, wheat, barley, and maize, from this wheat, is the highest product which is cover approximately half of the agricultural land [41].

2.2. Methodological framework

This study used METRIC and SEBAL models to calculate evapotranspiration (ET) in an arid and semi-arid environment. Landsat (8) collection 1 level 2 and path 172 and row 039 of satellite data was acquired from USGS earth explorer (https://earthexplorer.usgs.gov/). The availability of meteorological data is a difficult task to calculate ET [42], and the site for weather data was obtained from (https://power.larc.nasa.gov/data-access-viewer/). The first step following downloading the Landsat image is converting by using the radiance rescaling factor from TOA (top of the atmosphere) to radiance [43,44]. The spectral radiance (Lb) for thermal radiation is computed from the digital number of each 30 m pixel. Spectral radiance is the outgoing radiation energy of the band as observed at the top of the atmosphere by the satellite [45].

The spectral radiance (Lb) for thermal radiation is computed as demonstrated in Fig. 2:

$$\mathrm{Lb} = \left(\frac{L_{\max} - L_{\min}}{\mathrm{QCAL}_{\max} - \mathrm{QCAL}_{\min}}\right) \times \left(\mathrm{DN} - \mathrm{QCAL}_{\min}\right) + L_{\min} \quad (1)$$

where DN is the digital number of each pixel (recall that DN is used to efficiently "pack" data for transmission from the satellite), and $L_{\max}$ and $L_{\min}$ are calibration constants found in the header file. These represent the maximum and minimum radiance values used to scale the DN [46]. $L_{\max}$ and $L_{\min}$ will have the same dimensions as Lb and W/m^2/sr/μm. The QCA$L_{\max}$ and QCA$L_{\min}$ are the highest and lowest range of values for rescaled radiance in DN and are also found in the header file [47].

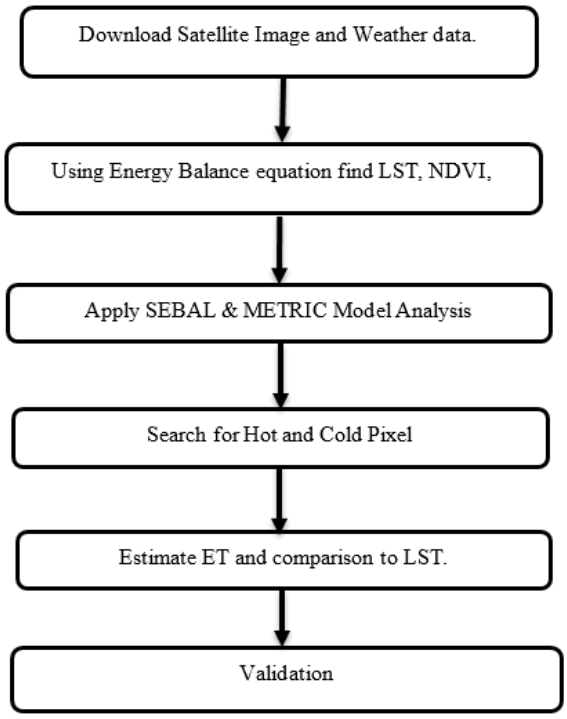

Fig. 2. General flow chart for the methodology.

Secondly conversion to TOA to TB (temperature brightness) and Lb (spectral radiance data) [47]. This can be changed to the temperature brightness of the top of the atmosphere by using metadata of thermal constant [48].

$$\mathrm{TB} = \frac{K_2}{\ln\left(k_1 / L\lambda + 1\right)} \quad (2)$$

Normalized differential vegetation index (NDVI) is calculated by using (Band 5) or (near infrared) and (Band 4) or red.

$$\mathrm{NDVI} = \frac{\left(\mathrm{NIR} - \mathrm{RED}\right)}{\left(\mathrm{NIR} + \mathrm{RED}\right)} \quad (3)$$

Thirdly emissivity is calculated from the NDVI data. This narrow band emissivity is expressed as εN [49]:

$$\mathrm{PV} = \frac{\left(\mathrm{NDVI} - \mathrm{NDVI}_{\min}\right)}{\left(\mathrm{NDVI}_{\max} - \mathrm{NDVI}_{\min}\right)^2} \quad (4)$$

For NDVI > 0
εNB = 0.97 + 0.0033 LAI; for LAI ≤ 3
εNB = 0.98 for LAI > 3
For NDVI ≤ 0

$$\text{Water, albedo}\left(\alpha\right) > 0.47,\ \varepsilon\mathrm{NB} = 0.99 \text{ and } \epsilon_0 = 0.985 \quad (5)$$

where PV – proportion of vegetation, NDVI, DN values from NDVI image, $\mathrm{NDVI}_{\min}$, minimum DN values from NDVI image, $\mathrm{NDVI}_{\max}$, maximum DN values from NDVI image. The leaf area index (LAI) is the proportion between the plant leaves found in all areas to the area on the ground characterized by the plant, in which the value ranges between 0 to 6. The leaf area index is a dimensionless ratio of m^2 by m^2 [50].

$$\begin{aligned} &\mathrm{LAI} = 11.\mathrm{SAVI}^3; && \text{for SAVI} \le 0.817 \\ &\mathrm{LAI} = 6; && \text{for SAVI} \ge 0.817 \end{aligned} \quad (6)$$

where SAVI is the Soil Adjusted Vegetation Index.

And then calculating LST the land surface temperature, which means temperature gain from radiative. This can be obtained using the temperature brightness of TOA and emitted radiance wavelength.

$$\mathrm{LST} = \frac{K_2}{\ln\left(\frac{\varepsilon_{\mathrm{NB}} \times K_1}{R_c} + 1\right)} \quad (7)$$

$$\mathrm{LST} = \frac{\mathrm{BT}}{\left(1+\left(\lambda \mathrm{BT}/c_2\right)\ln\left(E\right)\right)} \tag{8}$$

where LST surface temperature, K_1, and K_2 are constant values obtained from metadata of Landsat (8) image, R_c is the thermal radiance corrected from the surface where: LST is the surface temperature (K), R_c is the corrected thermal radiance, and calculated from λl using atmospheric standard correction.

Finally, the image was processed by LandMOD ET mapper, which is a MATLAB-based software (GUI) for the application of METRIC and SEBAL models on MODIS and Landsat images [16] using different input files such as remote sensing files, Weather and derived product that shows features of earth surface and cloud information such as surface roughness, cloud information, agriculture and water bodies.

Land surface temperature, albedo, NDVI, and emissivity are examples of remote sensing inputs (Fig. 3). All of these input files are unitless except LST with a unit in K whereas weather input files such as relative humidity (%), daily solar radiation (W/m^2), daily wind speed (m/s), and air temperature (K).

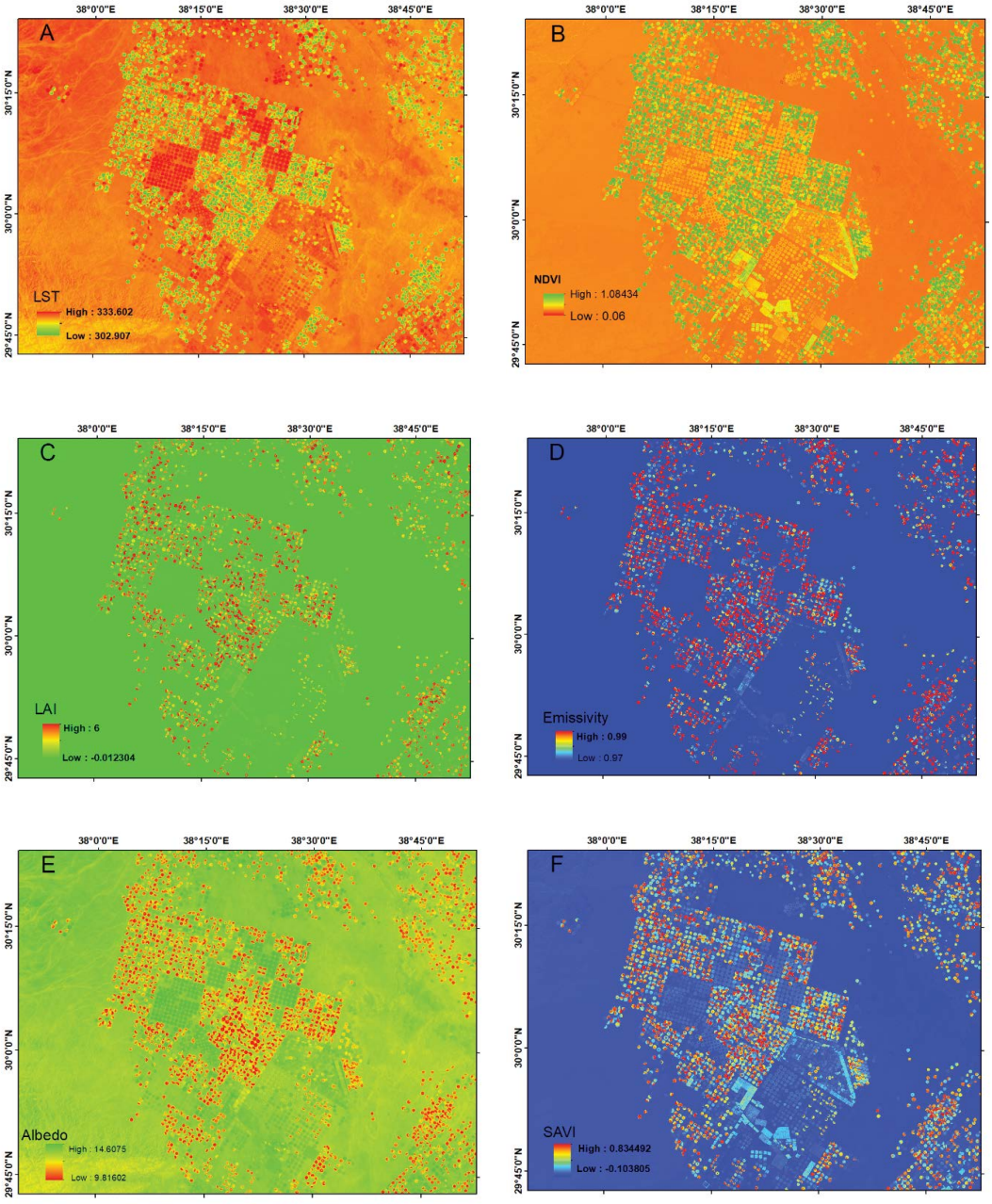

Fig. 3. (A) Land surface temperature, (B) normalized differential vegetation index, (C) leaf area index, (D) emissivity, (E) surface albedo and (F) SAVI.

The relation between ETr (actual evaporation) and flux, that is, nR (net radiation), Hi (sensible heat flux), Gi (soil heat flux), Le (latent heat flux) [51] are:

$$L_E = nR - \mathrm{Gi} - \mathrm{Hi} \tag{9}$$

$$\mathrm{ETr} = 3{,}600 \cdot \frac{L_E}{\lambda \sigma_w} \tag{10}$$

The daily values of ET (24) have more important and applicable than the instantaneous amount [52] SEBAL calculate the ET24 amount assuming instantaneous ETrF is similar to mean ETrF throughout 24 h. The value of ETrF (mm/d) is obtained as [12,53].

$$\mathrm{ET24} = \mathrm{ETrF} \times \mathrm{ETr}_{24} \tag{11}$$

3. Result and discussion

The value of ETr varies based on climate, vegetation cover, soil moisture condition, land use, and land cover and management practices [15]. Several results showed the highest ET from cropland areas [15]. According to Fig. 4, the value of fractional ET ranges from 0.001 to 1.1 mm/d and LST ranges between 302.9 to 333.6 K. The high mountain and agriculture part showed the highest amount of ET and whereas the low elevated region showed a low value of land surface temperature, which cover most of the north easter part of the region. The satellite images acquired on 2019/07/07 show a strong link between fractional ET and land surface temperature, with $R^2 = 0.8$.

The model output shown in Fig. 4 during the process of LandMOD ET mapper toolbox is ET in (mm/d), instantaneous of (ET (mm/h), sensible heat flux in (W/m^2 latent heat flux in (W/m^2) and net radiative flux in W/m^2)) [16]. The METRIC model was also used to estimate latent heat flux [54]. The relatively high value of daily evapotranspiration was obtained due to sensible heat flux, which is the main portion of energy, whereas the latent heat flux is dominated only by the vegetable and agricultural area [7,55].

The estimation of ETr was conducted after calculating flux such as latent heat flux of instantaneous evaporation, net radiation flux (Ri), sensible radiation flux (Hi), and soil heat flux (Gi) [13] as shown in Fig. 5. The value of ET estimated using Landsat data of both models ranges from 0.05 to 8 mm during 2019/07/07. This highly elevated agricultural area (Fig. 6.) shows a high value of ET ranging from 5 to 8 mm/d. This indicates that Agricultural and hilly terrain specifically in Arid and semi-arid environment results in a high value of ET. The scatter plot between DailyMETRIC and DailySEBAL models shows with R^2 = 0.7 (Fig. 6). The highest evapotranspiration values are shown in the red mark and that

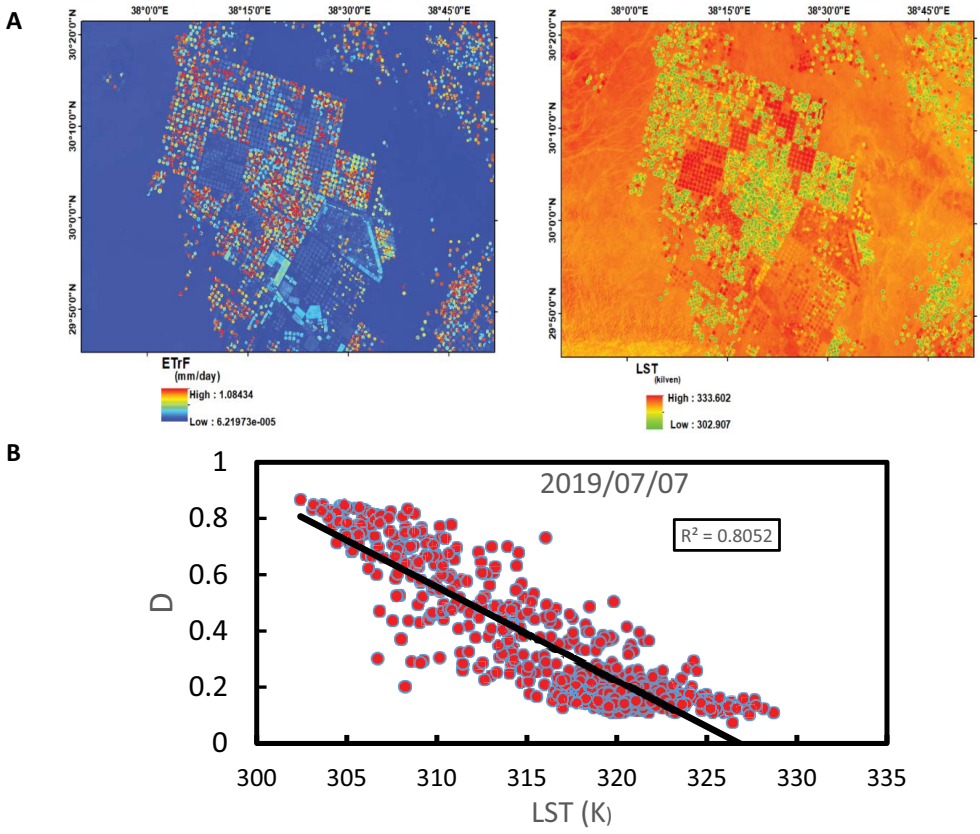

Fig. 4. (A) Daily reference evapotranspiration maps of the study area (mm/d) during 2019/07/07 and (B) comparison between land surface temperature and fractional evapotranspiration.

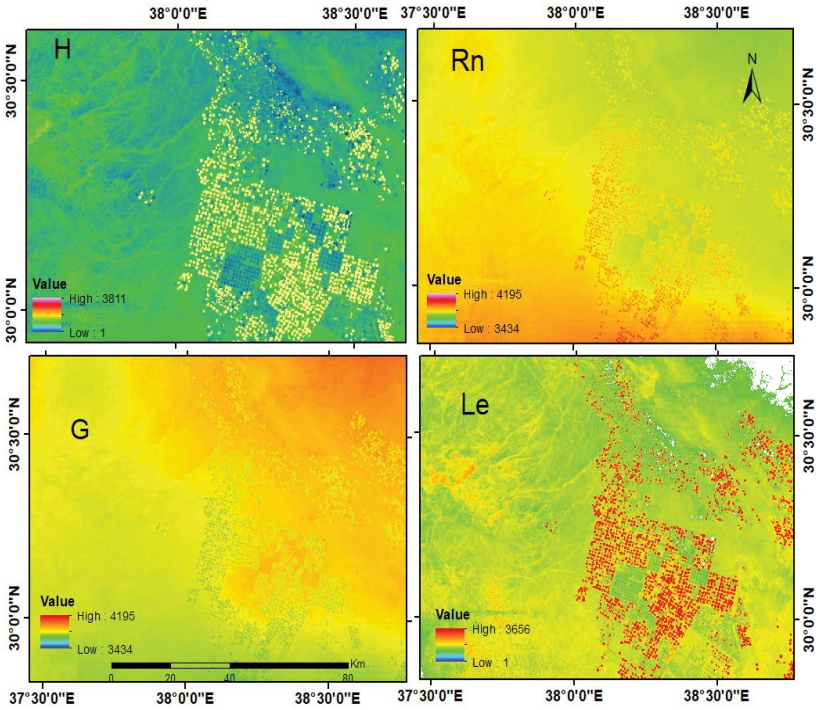

Fig. 5. Daily flux (W/m²) Le (latent heat flux), (H) sensible heat flux, (Rn) net radiative flux, and (Gi) soil heat flux.

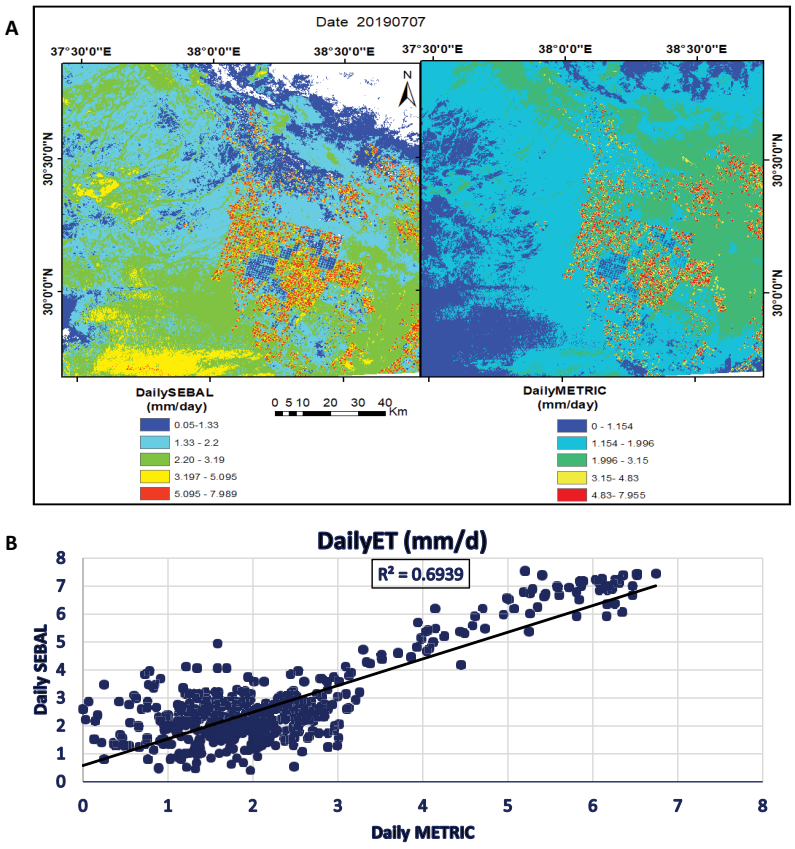

Fig. 6. (A) Daily evapotranspiration maps of the study area (mm/d) during 2019/07/07 and (B) comparison between daily METRIC and SEBAL model.

implies an agricultural pivoted area [56] as demonstrated in Fig. 6.

The distribution of ET depends on the feature of land cover and the result shows that the area in which low temperature and high NDVI value have high estimation of ETr and vice versa is shown in Fig. 4. A higher correlation has been observed between land surface temperature and evapotranspiration [57,58].

3.1. Model evaluation and comparison

Statical analysis (R^2) were performed for comparison between vegetation indices and ET derived from the METRIC and SEBAL model. The value of indices ranges between –0.5 to 0.87 for NDVI, from 0.43 to 0.84 for SAVI, from –0.8 to 6 for LAI, and from –0.77 to 0.453 for NDVI. Table 1 and Fig. 8 show the relationship and comparison between vegetation index and ET from both models. The value of R^2 ranges from 0.7049 to 0.88 in all cases and a higher value of R^2 = 0.88 is observed between SAVI and ET from SEBAL. Therefore, a good correlation has been seen (R^2 > 0.81) for ET from the SEBAL model whereas for the METRIC model, the value ranges between 0.7 to 0.86. Generally, the value ET from the SEBAL model is better compared to the METRIC model based on R^2 of different vegetation indices (Fig. 7).

According to the scatter plot in Fig. 8, a linear relationship has been seen between ET and NDVI, and the SAVI

Table 1
Statistical (R^2) comparison of two models with vegetation index

Model	Normalized differential vegetation index	Leaf area index	SAVI	NDVI
Evapotranspiration from METRIC	0.8632	0.7449	0.7867	0.7049
Evapotranspiration from SEBAL	0.8772	0.8317	0.8814	0.8146

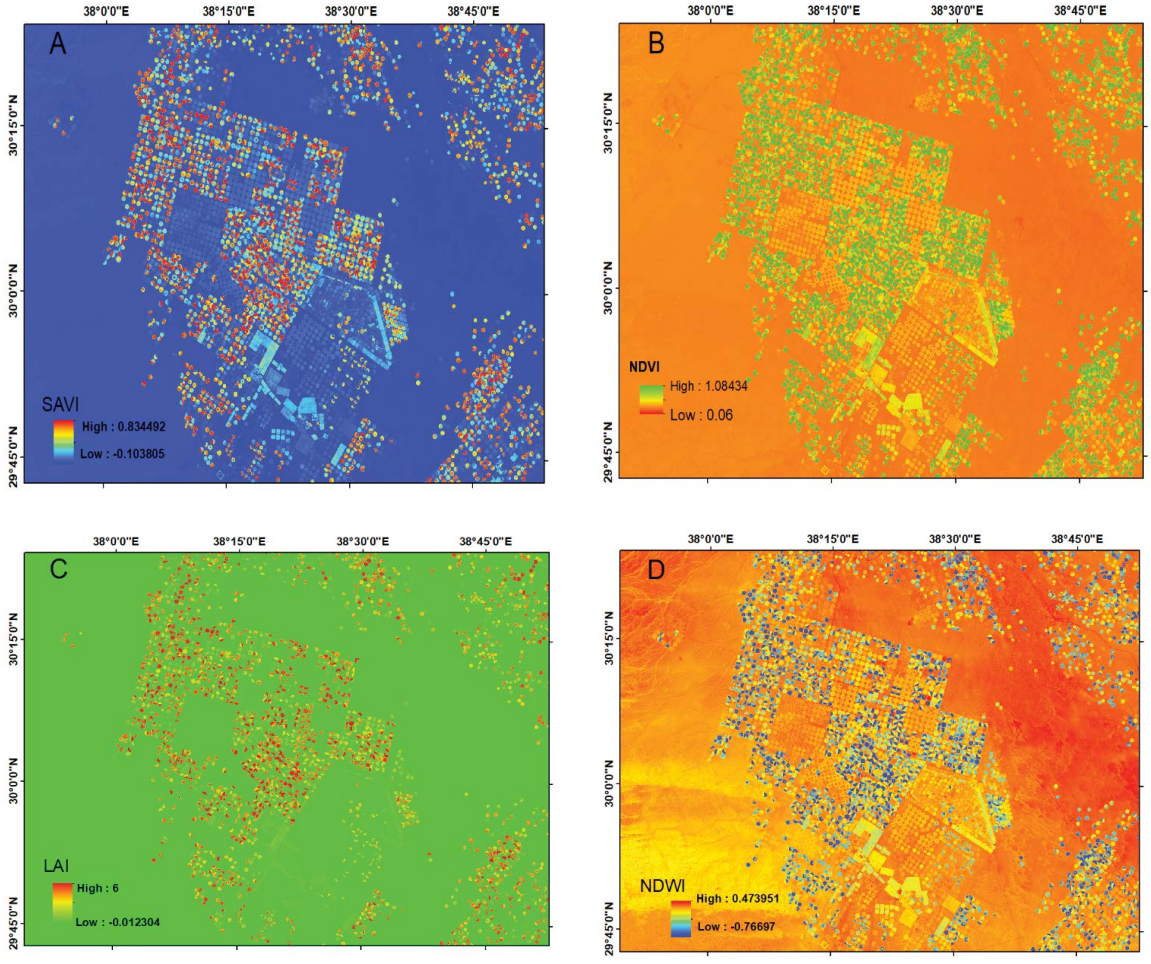

Fig. 7. Vegetation indices, (A) SAVI, (B) normalized differential vegetation index, (C) leaf area index, and (D) NDVI.

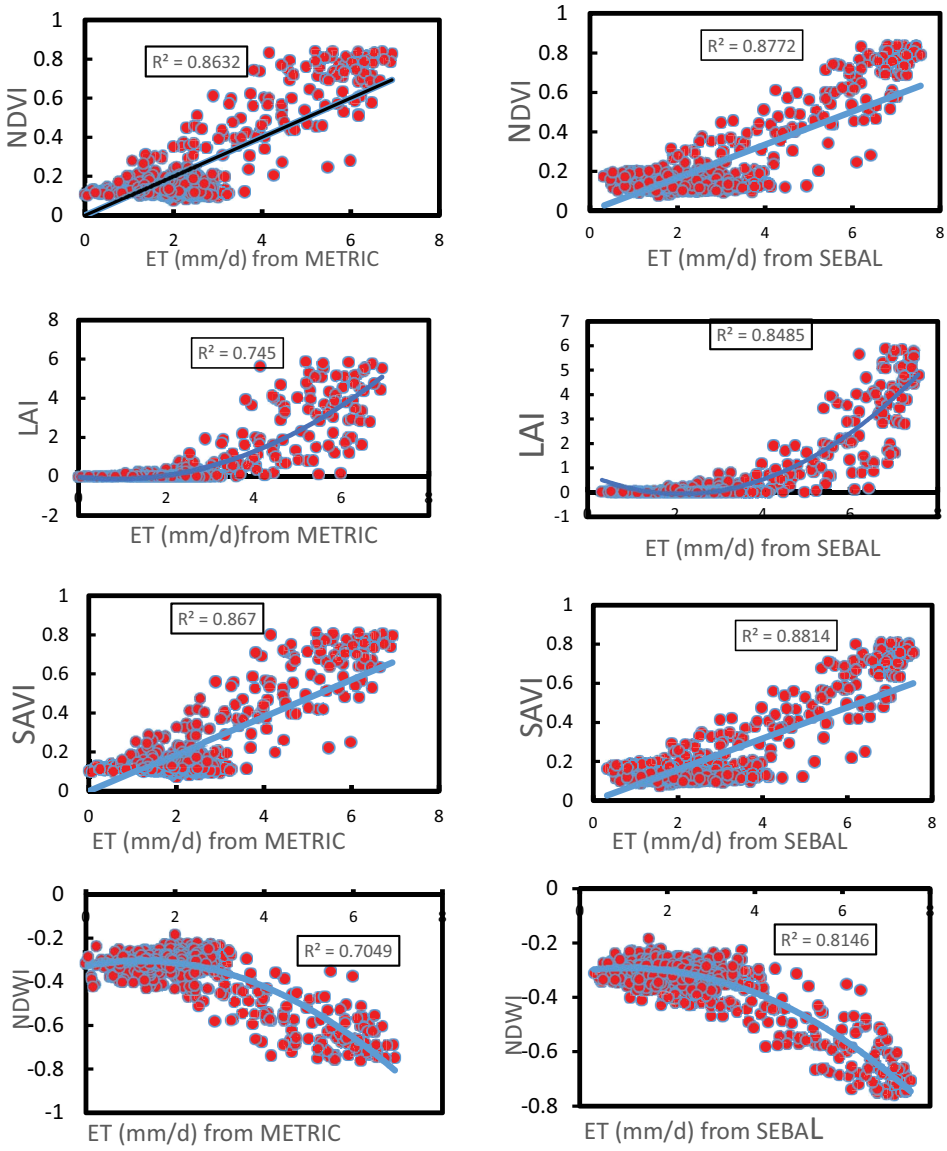

Fig. 8. Scatter plot between vegetation indices and evapotranspiration from METRIC and SEBAL model.

index. In addition, higher R^2 obtained for NDVI and SAVI comparable to the other. Exponential relation between LAI and ET was observed whereas for NDVI and ET inverse relation has been seen due to arid and sub-arid environments. Because NDVI is used to identify the land surface's water body feature. Hence the area is an arid and sub-arid environment due to the lack of water bodies, resulting in a highly inverse correlation (higher value R^2) obtained between NDVI and ET [59].

4. Conclusions

Using remote sensing data, this study presents a computational approach to assess and determine the daily ET quantity in and around the Al-Jouf region of Saudi Arabia. The result shows there is a highly inverse relation between fractional ET values and land surface temperature. The benefits of satellite remote sensing in estimating and analyzing evapotranspiration are typically important in irrigation, hydrology, and water resource management. The image is processed by LandMOD ET mapper, which is a MATLAB-based GUI for the application of METRIC and SEBAL models on Landsat and MODIS [16]. The hourly and daily actual ET was estimated for SEBAL and METRIC models. The area average evapotranspiration is about 2.21 mm/d for the METRIC model, and 2.6 mm/d for SEBAL (Fig. 6). According to [56] high value of ET is considered for an arid environment. The average land surface temperature is 324.3 K. The range of ET estimated using the SEBAL model is 0.05–8 mm. Higher Et value is shown in high mountains and agricultural areas this is due to the environmental condition being arid and semiarid. Studies show in the Nile delta agricultural region, which is located in the center, has the greatest daily evapotranspiration values calculated

from SEBS model results around 2.5 mm/d [38] which is a nearly similar result obtained in our studies.

The results demonstrated the capability of automated METRIC and SEBAL models to operate using various energy fluxes, including Le (latent heat flux), H (sensible heat flow), Rn (net radiative flux), and Gi (soil heat flux). Statical analysis (R^2) were performed for comparison between vegetation indices and ET derived from the METRIC and SEBAL model. The value of indices ranges between –0.5 to 0.87 for NDVI, from 0.43 to 0.84 for SAVI, from –0.8 to 6 for LAI, and from –0.77 to 0.453 for NDVI.

Generally, based on the map and correlation plot (Fig. 4) high value of R^2 = 0.8 is observed between ET and land surface temperature. For ET and other vegetation indices, R^2 was larger than 0.7. This is due to the METRIC model has highly dependent on weather data than SEBAL. Compared to the METRIC model, the SEBAL model is significantly more closely tied to the vegetation index.

Funding

The authors declare that no funds, grants, or other support were received during the preparation of this manuscript yet.

Competing interests

The authors have no relevant financial or non-financial interests to disclose.

Author contributions

Esubalew Adem: data collection and analysis (yibrie@gmail.com);

Silvena Boteva: verification and accuracy assessment (silvenab@abv.bg);

Lifu Zhang: data analysis (zhanglf@radi.ac.cn);

Mohamed Elhag: conceptualization and draft editing (melhag@kau.edu.sa);

All authors read and approved the final manuscript.

References

[1] H. Salimi, E. Asadi, S. Darbandi, Meteorological and hydrological drought monitoring using several drought indices, Appl. Water Sci., 11 (2021) 1–10.
[2] J. Zhao, C. Li, T. Yang, Y. Tang, Y. Yin, X. Luan, S. Sun, Estimation of high spatiotemporal resolution actual evapotranspiration by combining the SWH model with the METRIC model, J. Hydrol., 586 (2020) 124883, doi: 10.1016/j.jhydrol.2020.124883.
[3] Z. Chen, Z. Zhu, H. Jiang, S. Sun, Estimating daily reference evapotranspiration based on limited meteorological data using deep learning and classical machine learning methods, J. Hydrol., 591 (2020) 125286, doi: 10.1016/j.jhydrol.2020.125286.
[4] V. Burchard-Levine, H. Nieto, D. Riaño, W.P. Kustas, M. Migliavacca, T.S. El-Madany, J.A. Nelson, A. Andreu, A. Carrara, J. Beringer, A remote sensing-based three-source energy balance model to improve global estimations of evapotranspiration in semi-arid tree-grass ecosystems, Global Change Biol., 28 (2022) 1493–1515.
[5] M. Tasumi, Estimating evapotranspiration using METRIC model and Landsat data for better understandings of regional hydrology in the western Urmia Lake Basin, Agric. Water Manage., 226 (2019) 105805, doi: 10.1016/j.agwat.2019.105805.
[6] H.M. Al-Ghobari, Estimation of reference evapotranspiration for southern region of Saudi Arabia, Agric. For. Meteorol., 19 (2000) 81–86.
[7] M. Elhag, Sensitivity analysis assessment of remotely based vegetation indices to improve water resources management, Environ. Dev. Sustainability, 16 (2014) 1209–1222.
[8] T. Govender, T. Dube, C. Shoko, Remote sensing of land use-land cover change and climate variability on hydrological processes in Sub-Saharan Africa: key scientific strides and challenges, Geocarto Int., 38 (2022) 1–25.
[9] M.H. Jahangir, M. Arast, Remote sensing products for predicting actual evapotranspiration and water stress footprints under different land cover, J. Cleaner Prod., 266 (2020) 121818, doi: 10.1016/j.jclepro.2020.121818.
[10] R.G. Allen, M. Tasumi, R. Trezza, Satellite-based energy balance for mapping evapotranspiration with internalized calibration (METRIC)—model, Hydrol. Processes, 133 (2007) 380–394.
[11] M.C. Anderson, R.G. Allen, A. Morse, W.P. Kustas, Use of Landsat thermal imagery in monitoring evapotranspiration and managing water resources, Remote Sens. Environ., 122 (2012) 50–65.
[12] R. Allen, A. Irmak, R. Trezza, J.M. Hendrickx, W. Bastiaanssen, J. Kjaersgaard, Satellite-based ET estimation in agriculture using SEBAL and METRIC, Hydrol. Processes, 25 (2011) 4011–4027.
[13] H. Nouri, M. Faramarzi, B. Sobhani, S. Sadeghi, Estimation of evapotranspiration based on Surface Energy Balance Algorithm for Land (SEBAL) using Landsat 8 and MODIS images, Appl. Ecol. Environ. Res., 15 (2017) 1971–1982.
[14] R.G. Allen, C. Morton, B. Kamble, A. Kilic, J. Huntington, D. Thau, N. Gorelick, T. Erickson, R. Moore, R. Trezza, EEFlux: A Landsat-Based Evapotranspiration Mapping Tool on the Google Earth Engine, 2015 ASABE/IA Irrigation Symposium: Emerging Technologies for Sustainable Irrigation-A Tribute to the Career of Terry Howell, Sr. Conference Proceedings, 2015, pp. 1–11.
[15] G.B. Senay, M. Friedrichs, R.K. Singh, N.M. Velpuri, Evaluating Landsat 8 evapotranspiration for water use mapping in the Colorado River Basin, Remote Sens. Environ., 185 (2016) 171–185.
[16] N. Bhattarai, L.J. Quackenbush, J. Im, S.B. Shaw, A new optimized algorithm for automating endmember pixel selection in the SEBAL and METRIC models, Remote Sens. Environ., 196 (2017) 178–192.
[17] J.M. Ramírez-Cuesta, R.G. Allen, D.S. Intrigliolo, A. Kilic, C. Robison, R. Trezza, C. Santos, I.J. Lorite, METRIC-GIS: an advanced energy balance model for computing crop evapotranspiration in a GIS environment, Environ. Modell. Software, 131 (2020) 104770, doi: 10.1016/j.envsoft.2020.104770.
[18] D. Guo, S. Westra, H.R. Maier, An R package for modelling actual, potential and reference evapotranspiration, Environ. Modell. Software, 78 (2016) 216–224.
[19] G.F. Olmedo, S. Ortega Farias, D. Fonseca Luengo, F. Fuentes Peñailillo, Water: tools and functions to estimate actual evapotranspiración using Land Surface Energy Balance Models in R, The R J., 2 (2016) 352–369.
[20] L.B. Ferreira, F.F. da Cunha, Multi-step ahead forecasting of daily reference evapotranspiration using deep learning, Comput. Electron. Agric., 178 (2020) 105728, doi: 10.1016/j.compag.2020.105728.
[21] M. He, J.S. Kimball, Y. Yi, S.W. Running, K. Guan, A. Moreno, X. Wu, M. Maneta, Satellite data-driven modeling of field scale evapotranspiration in croplands using the MOD16 algorithm framework, Remote Sens. Environ., 230 (2019) 111201, doi: 10.1016/j.rse.2019.05.020.
[22] Z. Su, The Surface Energy Balance System (SEBS) for estimation of turbulent heat fluxes, Hydrol. Earth Syst. Sci., 6 (2002) 85–100.
[23] R.K. Singh, A. Irmak, S. Irmak, D.L. Martin, Application of SEBAL model for mapping evapotranspiration and estimating surface energy fluxes in south-central Nebraska, J. Irrig. Drain. Eng., 134 (2008) 273–285.

[24] W. Bastiaanssen, B. Thoreson, B. Clark, G. Davids, Discussion of "Application of SEBAL model for mapping evapotranspiration and estimating surface energy fluxes in south-central Nebraska" by Ramesh K. Singh, Ayse Irmak, Suat Irmak, and Derrel L. Martin, J. Irrig. Drain. Eng., 136 (2010) 282–283.
[25] F. Mohammed, A. Elfeki, M. Elhag, A. Chaabani, A comparative study of the estimation methods for NRCS curve number of natural arid basins and the impact on flash flood predications, Arabian J. Geosci., 14 (2021) 1–23.
[26] A. Irmak, R.G. Allen, J. Kjaersgaard, J. Huntington, B. Kamble, R. Trezza, I. Ratcliffe, Operational remote sensing of ET and challenges, Remote Sens. Environ., (2012) 467–492.
[27] M. Elhag, Inconsistencies of SEBS model output based on the model inputs: global sensitivity contemplations, J. Indian Soc. Remote Sens., 44 (2016) 435–442.
[28] S. Hussain, A.M. Elfeki, A. Chaabani, E.A. Yibrie, M. Elhag, Spatio-temporal evaluation of remote sensing rainfall data of TRMM satellite over the Kingdom of Saudi Arabia, Theor. Appl. Climatol., 150 (2022) 363–377.
[29] W. Senkondo, S.E. Munishi, M. Tumbo, J. Nobert, S.W. Lyon, Comparing remotely-sensed surface energy balance evapotranspiration estimates in heterogeneous and data-limited regions: a case study of Tanzania's Kilombero Valley, Remote Sens., 11 (2019) 1289, doi: 10.3390/rs11111289.
[30] S. Ortega, Evaluation of the METRIC Model for Mapping Energy Balance Components and Actual Evapotranspiration for a Super-Intensive Drip-Irrigated Olive Orchard, Dissertations & Theses in Natural Resources, 2019, p. 296.
[31] B. Jarbou, A. Alqarawy, A. Chabaani, A. Elfeki, M. Elhag, Spatiotemporal analysis of the annual rainfall in the Kingdom of Saudi Arabia: predictions to 2030 with different confidence levels, Theor. Appl. Climatol., 146 (2021) 1479–1499.
[32] S. Islam, R.A. Khan, M. Ahmad, M. Al Qahtani, Computation of potential evapo-transpiration under different climatic condition, Kingdom of Saudi Arabia, Int. J. Eng. Assoc., 4 (2015) 107–111.
[33] A.M. Youssef, S.A. Sefry, B. Pradhan, E.A. Alfadail, Analysis on causes of flash flood in Jeddah city (Kingdom of Saudi Arabia) of 2009 and 2011 using multi-sensor remote sensing data and GIS, Geomatics Nat. Hazards Risk, 7 (2016) 1018–1042.
[34] F.M. Al Zawad, A. Aksakal, Impacts of Climate Change on Water Resources in Saudi Arabia, The 3rd International Conference on Water Resources and Arid Environments (2008) and the 1st Arab Water Forum, 2010, pp. 511–523.
[35] M. Elhag, J. Bahrawi, S. Boteva, Input/output inconsistencies of daily evapotranspiration conducted empirically using remote sensing data in arid environments, Open Geosci., 13 (2021) 321–334.
[36] J. Steiner, T. Howell, A. Schneider, Lysimetric evaluation of daily potential evapotranspiration models for grain sorghum, Agron. J., 83 (1991) 240–247.
[37] R.K. Singh, S. Islam, R.A. Khan, M. Danish, Analysis of potential evapotranspiration of different cities of Kingdom of Saudi Arabia, J. Artif. Intell. Res., 5 (2015) 48–51.
[38] M. Elhag, A. Psilovikos, I. Manakos, K. Perakis, Application of the SEBS water balance model in estimating daily evapotranspiration and evaporative fraction from remote sensing data over the Nile Delta, Water Resour. Manage., 25 (2011) 2731–2742.
[39] S. Hussain, J. Bahrawi, M. Awais, M. Elhag, Understanding the role of the radiometric indices in temporal evapotranspiration estimation in arid environments, Desal. Water Treat., 256 (2022) 221–234.
[40] H. Nouri, S. Beecham, F. Kazemi, A. Hassanli, S. Anderson, Remote sensing techniques for predicting evapotranspiration from mixed vegetated surfaces, Hydrol. Earth Syst. Sci. Discuss., 10 (2013) 3897–3925.
[41] S. Chowdhury, M. Al-Zahrani, Implications of climate change on water resources in Saudi Arabia, Arabian J. Sci. Eng., 38 (2013) 1959–1971.
[42] L.B. Ferreira, F.F. da Cunha, R.A. de Oliveira, E.I. Fernandes Filho, Estimation of reference evapotranspiration in Brazil with limited meteorological data using ANN and SVM–a new approach, J. Hydrol., 572 (2019) 556–570.
[43] U. Avdan, G. Jovanovska, Algorithm for automated mapping of land surface temperature using Landsat 8 satellite data, J. Sens., 2016 (2016) 1–8.
[44] B. Kumari, M. Tayyab, J. Mallick, M.F. Khan, A. Rahman, Satellite-driven land surface temperature (LST) using Landsat 5, 7 (TM/ETM+ SLC) and Landsat 8 (OLI/TIRS) data and its association with built-up and green cover over urban Delhi, India, Remote Sens., 1 (2018) 63–78.
[45] G. Roerink, Z. Su, M. Menenti, S-SEBI: a simple remote sensing algorithm to estimate the surface energy balance, Phys. Chem. Earth Part B, 25 (2000) 147–157.
[46] J.G. Liu, P.J. Mason, Image Processing and GIS for Remote Sensing: Techniques and Applications, John Wiley & Sons, 2016.
[47] H. Oguz, LST calculator: a program for retrieving land surface temperature from Landsat TM/ETM+ imagery, Environ. Eng. Manage. J., 12 (2013) 549–555.
[48] A. Rajeshwari, N. Mani, Estimation of land surface temperature of Dindigul district using Landsat 8 data, Int. J. Eng. Res. Technol., 3 (2014) 122–126.
[49] N.P. Siddique, A. Ghaffar, Spatial and temporal relationship between NDVI and land surface temperature of Faisalabad city from 2000–2015, Eur. Online J. Nat. Soc., 8 (2019) 55–64.
[50] C.L. de Almeida, T.R.A. de Carvalho, J.C. de Araújo, Leaf area index of Caatinga biome and its relationship with hydrological and spectral variables, Agric. For. Meteorol., 279 (2019) 107705, doi: 10.1016/j.agrformet.2019.107705.
[51] J. Wang, T.W. Sammis, A.A. Andales, L.J. Simmons, V.P. Gutschick, D.R. Miller, Crop coefficients of open-canopy pecan orchards, Agric. Water Manage., 88 (2007) 253–262.
[52] H. Nouri, M. Faramarzi, B. Sobhani, S. Sadeghi, Estimation of evapotranspiration based on surface energy balance algorithm for land (SEBAL) using Landsat 8 and MODIS images, Appl. Ecol. Environ. Res., 15 (2017) 1971–1982.
[53] E. Nuaman, M. Elhag, J. Bahrawi, L. Zhang, H.F. Gabriel, K. Ur Rahman, Soil erosion modelling and accumulation using RUSLE and remote sensing techniques: case study Wadi Baysh, Kingdom of Saudi Arabia, Sustainability, 15 (2023) 3218–3232.
[54] M. Taheri, M. Gholizadeh, M. Nasseri, B. Zahraie, H. Poorsepahy-Samian, V. Espanmanesh, Performance evaluation of various evapotranspiration modeling scenarios based on METRIC method and climatic indexes, Environ. Monit. Assess., 193 (2021) 1–18.
[55] C.M. Frey, E. Parlow, R. Vogt, M. Harhash, M.M. Abdel Wahab, Flux measurements in Cairo. Part 1: *in situ* measurements and their applicability for comparison with satellite data, Int. J. Climatol., 31 (2011) 218–231.
[56] M. Elhag, J.A. Bahrawi, Realization of daily evapotranspiration in arid ecosystems based on remote sensing techniques, Geosci. Instrum. Methods Data Syst., 6 (2017) 141–147.
[57] M. Elhag, I. Gitas, A. Othman, J. Bahrawi, A. Psilovikos, N. Al-Amri, Time series analysis of remotely sensed water quality parameters in arid environments, Saudi Arabia, Environ. Dev. Sustainability, 23 (2021) 1392–1410.
[58] A.Y. Aldhebiani, M. Elhag, A.K. Hegazy, H.K. Galal, N.S. Mufareh, Consideration of NDVI thematic changes in density analysis and floristic composition of Wadi Yalamlam, Saudi Arabia, Geosci. Instrum. Methods Data Syst., 7 (2018) 297–306.
[59] A. Psilovikos, M. Elhag, Forecasting of remotely sensed daily evapotranspiration data over Nile Delta region, Egypt, Water Resour. Manage., 27 (2013) 4115–4130.